Rotating Shadowband Radiometer Development and Analysis of Spectral Shortwave Data

J. Michalsky, L. Harrison, Q. Min, J. Schlemmer, W. Berkheiser III, and C. Zhou
Atmospheric Sciences Research Center
University at Albany, State University of New York
Albany, New York

Introduction

Our goals in the Atmospheric Radiation Measurement (ARM) Program are improved measurements of spectral shortwave radiation and improved techniques for the retrieval of climatologically sensitive parameters.

The mulifilter rotating shadowband radiometer (MFRSR) that was developed during the first years of the ARM program has become a workhorse at the Southern Great Plains (SGP) Cloud and Radiation Testbed (CART) site, and it is widely deployed in other climate programs. We have spent most of our effort this year developing techniques to retrieve column aerosol, water vapor, and ozone from direct beam spectral measurements of the MFRSR. Additionally, we have had some success in calculating shortwave surface albedo and aerosol optical depth from the ratio of direct to diffuse spectral irradiance. Using the surface albedo and the global irradiance, we have calculated cloud optical depths. From cloud optical depth and liquid water measured with the microwave radiometer, we have calculated effective liquid cloud particle radii.

The rest of the text will provide some detail regarding each of these efforts.

Aerosol Optical Depth

Five of the six filters in an MFRSR may be used for the measurement of aerosol optical depth. When the atmosphere is clear and stable, Langley analysis is possible. The Bouguer-Lambert-Beer law is given by

$$I = I_o e^{-\tau * m} \tag{1}$$

where I is the spectral irradiance as measured by the MFRSR, I_o is the spectral irradiance that the MFRSR would measure at the top of the atmosphere, τ is the total optical depth from all sources of extinction, and *m* is the air mass relative to the zenith direction. If the atmosphere is stable, a plot of the natural log of I versus *m* yields a linear plot whose slope is the total optical depth τ. The five filters that we use for aerosol measurements are sensitive to aerosol scattering/absorption and Rayleigh scattering at all wavelengths and to ozone absorption in three of the filters. Rayleigh scattering depends only on surface pressure and is easily subtracted. Ozone may either be measured independently or inferred from the data (which we discuss below) and subtracted. This yields the aerosol optical depth.

I_o may be obtained from a standard lamp or derived from Langley plots according to the above procedure on occasions when the atmosphere is stable. When the atmosphere is free of clouds, but unstable because of changing aerosol conditions, we may calculate τ using this measured I_o. We have used our estimate of I_o to calculate the averages of thirty-minute time series of optical depth. We allow the optical depth to change linearly in time, but if any point deviates by more than ± 0.01 optical depths from this linear behavior, we advance one time step and test the series again. When we find thirty minutes of data that satisfy the criterion, we advance thirty minutes and begin the search again. Figure 1 is a plot of daily averages of these thirty-minute samples. This daily average is used, rather than each thirty-minute sample, when looking for seasonal behavior because it does not preferentially weight the clearest days.

Water Vapor

Reagan et al. (1987) introduced the modified Langley technique as an independent method of calculating total column water vapor using the 940-nm water band in the near infrared. Bruegge et al. (1992) followed the Reagan method, but used LOWTRAN7 to calculate transmission in their water vapor passband. We have followed the procedure of Bruegge et al. (1992), but used MODTRAN2 for our transmission calculations. Derived water vapor column abundances for 104 clear mornings or afternoons have been compared to water vapor columns derived from microwave measurements made simultaneously at the SGP CART site central facility. These measurements

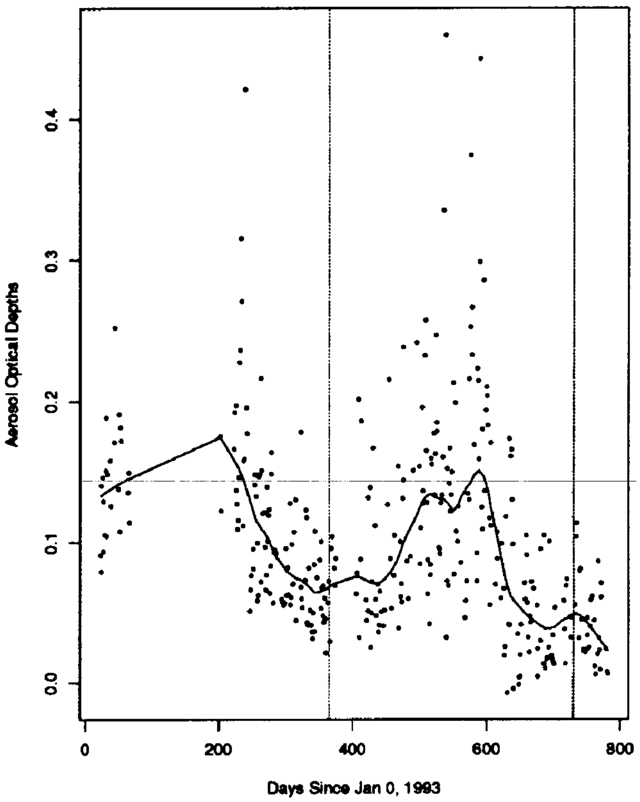

Figure 1. Daily-averaged aerosol optical depths at 500 nm for the SGP site central facility.

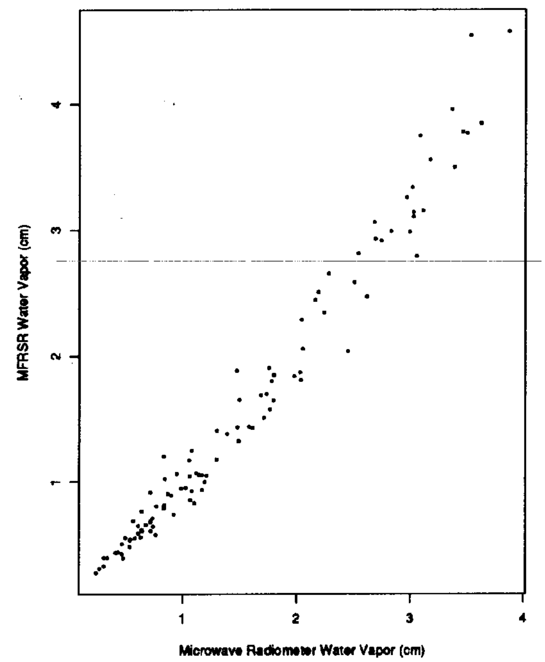

Figure 2. MFRSR-derived water vapor versus microwave radiometer water vapor at the SGP site.

span a year and cover the range of water vapor experienced at the SGP site. Figure 2 is a plot of the MFRSR-derived water vapor versus the microwave radiometer measurements for the same periods. At high water vapor the MFRSR reports slightly higher values than the microwave radiometer. At this point the slight discrepancy is not completely resolved.

Ozone

Ozone may also be derived using the five filters used in the aerosol optical depth derivation as suggested above. Realistic aerosol size distributions produce little curvature on a plot of the natural log of the aerosol optical depth versus the natural log of the wavelength for which the optical depth is obtained. This can be shown theoretically, and it is our experience experimentally. King and Byrne (1976) suggested that one could estimate this wavelength dependence with a quadratic function in these variables. By perturbing the ozone optical depth until a best quadratic fit is obtained, we can derive an estimate of ozone column abundance. Figure 3 is a plot of ozone column for the

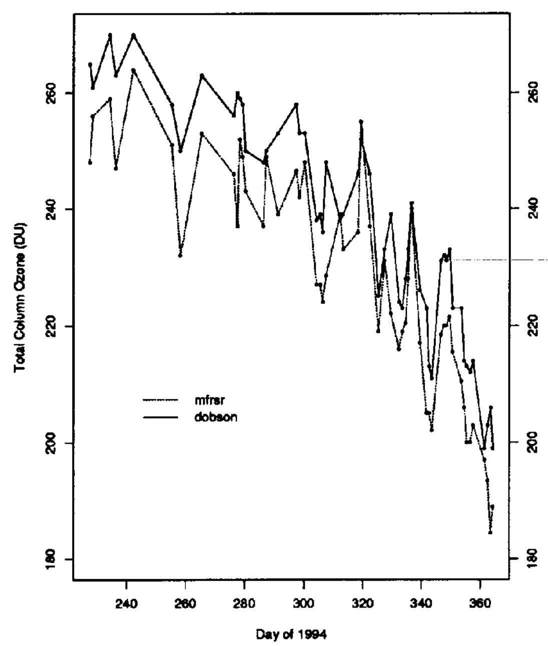

Figure 3. Mauna Loa Observatory total column ozone from the Dobson spectrometer and the MFRSR.

last four months of 1994 for the Dobson spectrophotometer at Mauna Loa Observatory and for the MFRSR. The Dobson is a standard for ozone measurements. The MFRSR data seem to follow closely but have a 10 Dobson-unit offset from the Dobson data. Filter stability is crucial for this technique to be valid, therefore we suspect the minor offset is associated with a filter shift. We will test this hypothesis further by recalibrating and by testing the method at other sites where standard ozone measurements are made and an MFRSR is acquiring data simultaneously.

Radiative Transfer and Surface Albedo

A certain amount of received solar radiation is multiply scattered, requiring a more rigorous treatment of scattering processes through the use of radiative transfer models that include all orders of multiple scattering. However, full radiative transfer computations are extremely time-consuming, limiting the applications of the radiative transfer model. Noting that the response of interest is merely the downward surface flux which is characterized by very large data bases (i.e., as a function of solar zenith angle), we developed the adjoint formulation of discrete ordinate radiative transfer to understand the measurements of the MFRSR.

Based on the definition of adjoint operator, $\langle I^*, LI \rangle = \langle L^*I^*, I \rangle$, we construct a variational principle for the forward radiative transfer equation. It leads to the adjoint formulation of the radiative transfer equation, $L^*I^* = F$, with appropriate boundary conditions. The adjoint operator is

$$L^*(z,\Omega) = -\mu\frac{d}{dz} + \beta^{ext} - \beta^{sca}\int_{4\pi} d\Omega' p(z, -\Omega' \to -\Omega) \qquad (2)$$

and the adjoint source for the downward diffuse irradiance is $\Sigma = -\mu\delta(z)U(-\mu)$. The downward diffuse irradiance, G[I], can be evaluated as

$$G[I] = \langle \Sigma, I \rangle = \langle L^*I^*, I \rangle = \langle I^*, LI \rangle = \langle I^*, Q \rangle \qquad (3)$$

The advantage of the adjoint method to evaluate the integral property is clearly demonstrated in the above equation. To calculate the radiative effects of *m* different sources, we must solve the forward radiative transfer equation *m* times. However, such effects can be evaluated by solving the adjoint radiative transfer equation once and undertaking *m* inner products instead.

The efficiency and accuracy of our adjoint method of radiative transfer are tested by comparing the results with the forward method of radiative transfer for a set of synthetic cases and for measurements with the MFRSR. It is demonstrated that the accuracy of the adjoint method is equal to that of the forward discrete ordinate radiative transfer method, and the computing time is significantly reduced.

The irradiance at the surface, as well as the diffuse/direct ratio, nonlinearly depends upon several factors such as wavelength, solar zenith angle, surface albedo, and atmospheric species including ozone, cloud, and aerosol. We employed the adjoint method of radiative transfer in conjunction with the nonlinear least squares method to infer the surface albedo and the aerosol optical depth simultaneously from the ratio of diffuse to direct irradiances.

We processed the data at wavelengths of 415, 500, 610, and 665 nm for the time intervals during which there is a clear stable atmosphere devoid of any cloud cover for a long enough period of time for the airmass to undergo a large change, particularly on the days in which the optical depths are large. We compared the inferred surface albedo with measurements at the SGP site of ARM and the inferred optical depth with the results of Langley regression. The data in Table 1 show reasonable agreement, when cloud-free conditions prevail.

Cloud Properties

Once the parameters related to surface albedo and aerosol have been retrieved, we can use the same approach to infer stratified cloud properties under cloud-covered sky. Specifying the single scattering albedo and the asymmetry factor based on Mie theory, we can infer the cloud optical depth from the global irradiance. We selected the transmittance of the atmosphere, the ratio of measured global irradiance to the solar constant, as the inversion function to avoid the uncertainties of absolute calibration.

We compared our inferred cloud optical depth with the Geostationary Operational Environmental Satellite (GOES) measurements at the SGP site during April 1994. Temporal variations of our results, shown in Figure 4, are consistent with that of GOES measurements. However, our results are slightly higher, which may be due to the effects of spatial average of GOES measurements over a 0.3° by 0.03° area.

Table 1. Summary of the observed and inferred surface albedo and total optical depth during August 1994 at SGP.						
		Surface Albedo			**Optical Depth**	
Time	**Wavelength λ(nm)**	**NLSM**	Λ_{10m}	Λ_{25m}	**NLSM**	**Langley Reg.**
940816	415	0.036±0.013	0.031	0.038	0.487±0.009	0.503±0.009
	500	0.066±0.011	0.048	0.063	0.285±0.006	0.299±0.004
	610	0.128±0.016	0.071	0.109	0.198±0.007	0.214±0.004
	665	0.162±0.019	0.079	0.126	0.144±0.007	0.162±0.004
940821	415	0.094±0.007	0.025	0.032	0.584±0.004	0.489±0.012
	500	0.088±0.007	0.045	0.052	0.372±0.004	0.373±0.004
	610	0.122±0.010	0.069	0.089	0.263±0.004	0.266±0.004
	665	0.137±0.009	0.074	0.105	0.197±0.004	0.207±0.004

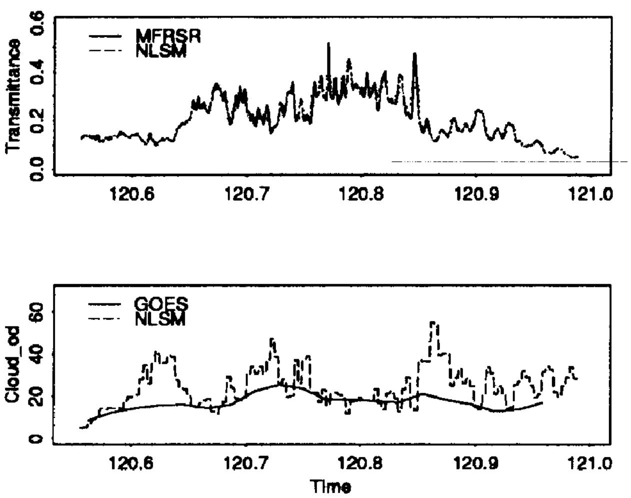

Figure 4. Measured and fitted transmittances and inferred cloud optical depths on April 30, 1994, at the SGP site.

Knowing the liquid water path from microwave radiometry, we can infer the effective radius of cloud drops through the relationship defined by Mie theory. We processed the data at the SGP site during August and September 1994. The inferred mean cloud particle radius and cloud optical depths are sensible. For example, on September 1, 1994, the inferred mean cloud particle radii vary from 4.2 µm to 12.8 µm as cloud optical depths vary from 16.0 to 91.8, respectively (Figure 5).

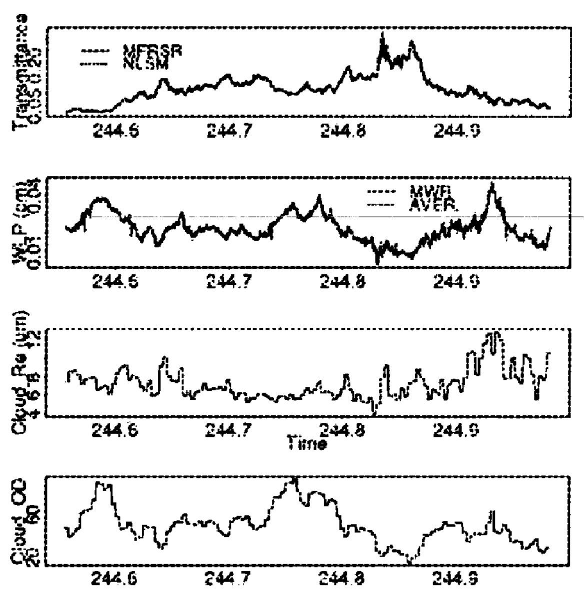

Figure 5. Transmittances, water liquid paths, inferred cloud effective radii, and cloud optical depths on Sept. 1, 1994, at the SGP site.

References

Bruegge, C. J., J. E. Conel, R. O. Green, J. S. Margolis, R. G. Holm, and G. Toon. 1992. Water vapor column abundance retrievals during FIFE, *J. Geophys. Res.*, **97(18)**, 759-768.

King, M. D., and D. M. Byrne. 1976. A method for inferring total ozone content from the spectral variation of total optical depth obtained with a solar radiometer, *J. Atmos. Sci.*, **33**, 2242-2251.

Reagan, J. A., K. Thome, B. Herman, and R. Gall. 1987. Water vapor measurements in the 0.94 micron absorption band. Calibration measurements, and data applications. In *Proceedings International Geoscience and Remote Sensing Symposium*, 1987 Symposium, Ann Arbor, Michigan, IEEE, pp. 63-67.